Cell

Follicular Dendritic Cells Emerge from Ubiquitous Perivascular Precursors

Nike Julia Krautler,[1,3,9] Veronika Kana,[1,9] Jan Kranich,[1] Yinghua Tian,[2] Dushan Perera,[1] Doreen Lemm,[1] Petra Schwarz,[1] Annika Armulik,[1] Jeffrey L. Browning,[4] Michelle Tallquist,[5] Thorsten Buch,[6] José B. Oliveira-Martins,[1] Caihong Zhu,[1] Mario Hermann,[1,7] Ulrich Wagner,[8] Robert Brink,[3] Mathias Heikenwalder,[1] and Adriano Aguzzi[1,*]

[1]Institute of Neuropathology
[2]Division of Visceral and Transplant Surgery
University Hospital of Zurich, 8091 Zurich, Switzerland
[3]Garvan Institute of Medical Research, Darlinghurst, New South Wales, Sydney 2010, Australia
[4]Biogen Idec, Immunobiology, 124 Cambridge Center, Cambridge, MA 02142, USA
[5]UT Southwestern Medical Center at Dallas, 5323 Harry Hines Boulevard, Dallas, TX 75390-9148, USA
[6]Institute of Experimental Immunology
[7]Institute of Laboratory Animal Science
University of Zurich, 8057 Zurich, Switzerland
[8]Ludwig Institute for Cancer Research, University of California San Diego, 9500 Gilman Drive, La Jolla, CA 92093, USA
[9]These authors contributed equally to this work
*Correspondence: adriano.aguzzi@usz.ch
http://dx.doi.org/10.1016/j.cell.2012.05.032

SUMMARY

The differentiation of follicular dendritic cells (FDC) is essential to the remarkable microanatomic plasticity of lymphoid follicles. Here we show that FDC arise from ubiquitous perivascular precursors (preFDC) expressing platelet-derived growth factor receptor β (PDGFRβ). PDGFRβ-Cre-driven reporter gene recombination resulted in FDC labeling, whereas conditional ablation of PDGFRβ$^+$-derived cells abolished FDC, indicating that FDC originate from PDGFRβ$^+$ cells. Lymphotoxin-α-overexpressing prion protein (PrP)$^+$ kidneys developed PrP$^+$ FDC after transplantation into PrP$^-$ mice, confirming that preFDC exist outside lymphoid organs. Adipose tissue-derived PDGFRβ$^+$ stromal-vascular cells responded to FDC maturation factors and, when transplanted into lymphotoxin β receptor (LTβR)$^-$ kidney capsules, differentiated into Mfge8$^+$CD21/35$^+$ FcγRIIβ$^+$PrP$^+$ FDC capable of trapping immune complexes and recruiting B cells. Spleens of lymphocyte-deficient mice contained perivascular PDGFRβ$^+$ FDC precursors whose expansion required both lymphoid tissue inducer (LTi) cells and lymphotoxin. The ubiquity of preFDC and their strategic location at blood vessels may explain the de novo generation of organized lymphoid tissue at sites of lymphocytic inflammation.

INTRODUCTION

Follicular dendritic cells (FDC) engage B cells in germinal centers (GC) of secondary lymphoid organs (SLO) with processes laced with immune complexes (IC) (Klaus et al., 1980; Mandel et al., 1980; Tew et al., 1982). B cells bearing high-affinity receptors for immune-complexed antigens establish contact with FDC, which in turn provide survival signals. FDC also supply milk-fat globule epidermal growth factor 8 (Mfge8, identical with the FDC-M1 antigen), which controls the engulfment of apoptotic B cells by macrophages (Hanayama et al., 2004; Kranich et al., 2008).

The origin of FDC is incompletely understood. FDC resemble fibroblasts ultrastructurally and appear to derive from local radioresistant precursors (Alimzhanov et al., 1997; Blättler et al., 1997; Cyster et al., 2000; Humphrey et al., 1984; Imazeki et al., 1992; Kamperdijk et al., 1978; Yoshida and Takaya, 1989). During chronic inflammatory reactions, which often result from impaired pathogen clearance (e.g., hepatitis C) or autoimmunity (e.g., rheumatoid arthritis), nonlymphoid tissues undergo reorganization into tertiary lymphoid tissues (TLT) (Aloisi and Pujol-Borrell, 2006; Drayton et al., 2006; Mebius, 2003). Similarly to SLO, TLT consist of highly structured T cell areas, B cell follicles, and FDC. TLT arise almost anywhere in the body, implying that FDC precursors may be ubiquitous.

Here we show that FDC are derived from ubiquitous perivascular PDGFRβ$^+$ precursors. Although the early perivascular progenitors are generated by a lymphotoxin (LT)-independent process, further maturation requires signaling by LT and tumor necrosis factor (TNF) family members. Beyond its relevance to SLO organogenesis, these findings help explaining the rapid generation of specialized TLT at virtually any vascularized site of chronic inflammation.

RESULTS

While investigating the cellular sources of splenic Mfge8 (FDC-M1), we noticed that *Mfge8* transcription was not restricted to mature FDC. It extended to cells located around marginal sinuses (MS) and within splenic T cell zones (Figure 1A) (Kranich

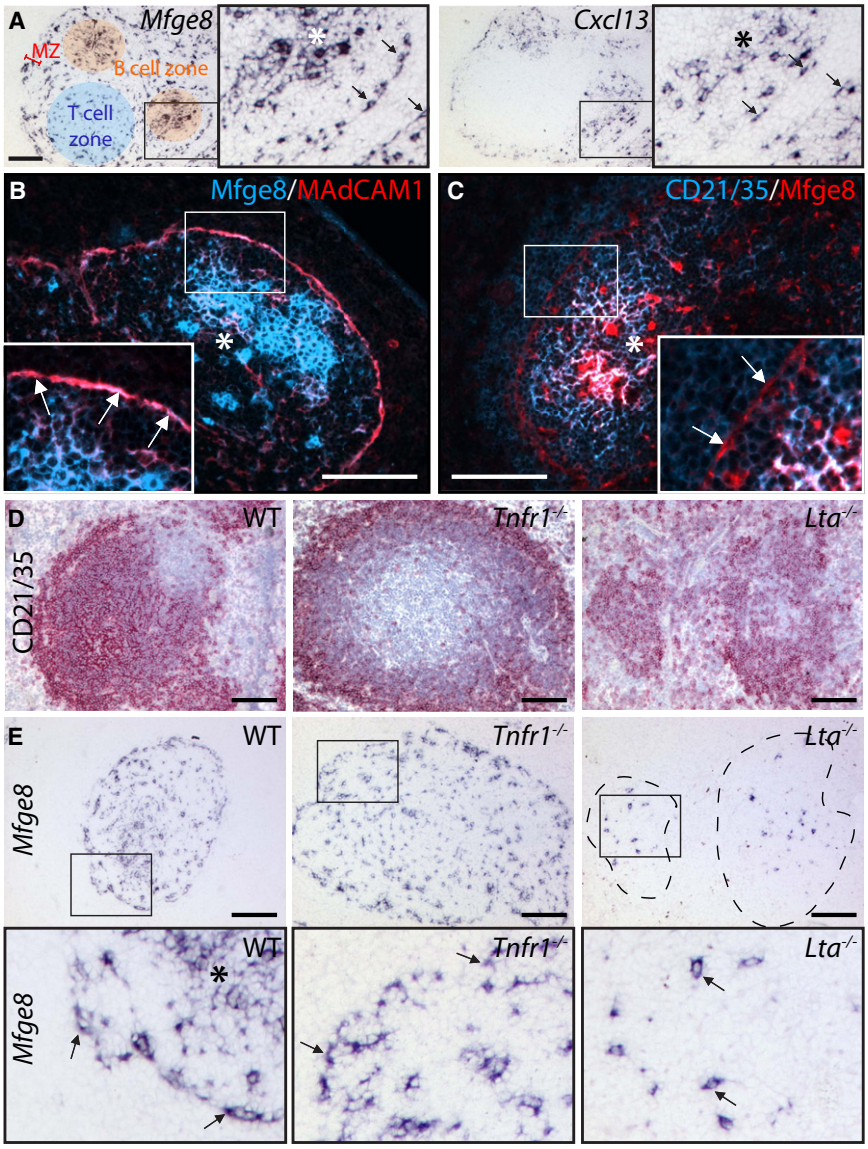

Figure 1. FDC-like Cells in Spleens Lacking FDC

(A) ISH for *Mfge8* and *Cxcl13* mRNA on consecutive WT spleen sections. Cellular compartments are highlighted in color: red, marginal zone (MZ); blue, T cell zone; orange, B cell follicle containing mature FDC. Boxes (here and henceforth): areas reproduced at higher resolution. Asterisks (here and henceforth): FDC networks in B cell follicle. Arrows: bipolar *Mfge8*$^+$ and *Cxcl13*$^+$ cells lining marginal sinuses (MS).

(B and C) IF stains for the FDC markers Mfge8 and MAdCAM1 (B) or CD21/35 (C) (Colocalization on mature FDC (asterisks), MS Mfge8$^+$ cells coexpress MAdCAM1 (arrows), but not CD21/35. Overlays of blue and red at similar intensity levels result in magenta, and higher-intensity blue yields a whitish signal.

(D and E) Consecutive sections of WT, *Tnfr1*$^{-/-}$, and *Lta*$^{-/-}$ spleens were analyzed for expression of *Mfge8* mRNA or stained for B cells and FDC with CD21/35. Arrows: *Mfge8*$^+$ cells in MS (WT and *Tnfr1*$^{-/-}$) and in white pulp (*Lta*$^{-/-}$). Dashed lines indicate margins of the vestigial follicles in the *Lta*$^{-/-}$ mice. Scale bar here and henceforth (unless indicated otherwise): 100 μm.

See also Figures S1 and S2.

et al., 2008) that often displayed two or more dendritic protrusions. In situ hybridization (ISH) for the FDC-associated chemokine CXCL13 (BLC) yielded similar patterns (Figure 1A). Mfge8$^+$ cells coexpressed MAdCAM1, ICAM1, and BP-3 (bone marrow stromal antigen 1) (Figure 1B; see S1A and S1B available online).

We then tested for the presence of CD21/35 and FcγRIIβ, which are instrumental to IC-trapping by FDC. However, no CD21/35 (Figure 1C) and very little FcγRIIβ were detectable by immunofluorescence (IF, Figure S1C). The prion protein (PrP), which is abundant on FDC, was also not detected (Figure S1D). Because they possessed some FDC-like properties yet lacked IC-trapping receptors, we considered these cells as immature and termed them "preFDC."

Activated macrophages can express *Mfge8* (Hanayama et al., 2002). We therefore investigated whether splenic Mfge8 originated from macrophages populating the marginal zone (MZ). However, the phagocytic markers ERTR-9 and MOMA-1 failed to colocalize with Mfge8 (Figures S1E and S1F). Moreover, reciprocal bone marrow (BM) chimeras between wild-type (WT) and *Mfge8*$^{-/-}$ mice had shown that all *Mfge8* transcribing cells within SLO were stromal and radioresistant (Kranich et al., 2008). Hence hematopoietic cells are not a source of Mfge8 within SLO.

preFDC Development Requires LTβR but Not TNFR1 Signaling

Sustained activation of the lymphotoxin beta receptor (LTβR) and the tumor necrosis factor receptor 1 (TNFR1) is required to induce and maintain FDC (De Togni et al., 1994; Fütterer et al., 1998; Le Hir et al., 1995–1996, 1996; Pasparakis et al., 1996). ISH analyses of spleens from mice lacking TNFR1 (Figures 1D, 1E, and S2A–S2C) or TNF alpha (*Tnfa*$^{-/-}$; data not shown) for *Mfge8* and *Cxcl13* revealed preserved preFDC in the MS and white pulp despite the absence of mature FDC and abnormal accumulations of CD21/35$^+$ B cells next to the MS (Figure 1D; Ngo et al., 1999). In contrast, ablation of LTβR or of its ligands (*Lta*$^{-/-}$, *Ltb*$^{-/-}$) decimated the preFDC population to single scattered cells within the disorganized white pulp (Figures 1D, 1E, and S2A–S2C).

These results suggest that the maintenance of preFDC relies on LTβR and their further maturation depends on TNFR1 signaling. We therefore treated WT mice with a soluble LTβR-Ig immunoadhesin (Force et al., 1995; Mackay and Browning, 1998; Ngo

et al., 1999). Upon intravenous treatment with LTβR-Ig, *Mfge8* expression was profoundly reduced in MS and T/B cell areas of these spleens compared to isotype-treated mice, confirming that LTβR signaling is also required by preFDC (Figure S2D).

preFDC in Mice Lacking Lymphocytes

FDC maturation strictly requires B cells expressing LTαβ (Fu et al., 1998; Tumanov et al., 2004). To define whether preFDC undergo B cell-dependent maturation stages, we analyzed *Mfge8* expression in μMT^D mice that lack B cells (Kitamura et al., 1991) and *Rag1*$^{-/-}$ mice that lack B and T cells (Mombaerts et al., 1992). Unexpectedly, ISH identified *Mfge8*$^+$ and *Cxcl13*$^+$ cells within the vestigial white pulp of μMT^D mice (Figure S3A) and even of *Rag1*$^{-/-}$ mice (Figure 2A and S3B; Ngo et al., 2001). We therefore investigated spleens of double mutants for Rag2 and the common cytokine receptor gamma chain (*Rag2*$^{-/-}\gamma c^{-/-}$) lacking B, T, and natural killer (NK) cells (Goldman et al., 1998). *Rag2*$^{-/-}\gamma c^{-/-}$ spleens had only few *Mfge8*$^+$/*Cxcl13*$^+$ clusters along isolectin B4 (IB4) positive vascular structures (Figures 2B, 2C, and S3C), whereas $\gamma c^{-/-}$ mice maintained *Mfge8*$^+$ FDC and preFDC (Figure S3D). *Rag2*$^{-/-}\gamma c^{-/-}$ *Mfge8*$^+$/*Cxcl13*$^+$ cells clustered along vessels stained for smooth muscle actin (SMA) and tyrosine hydroxylase (TH), reflecting innervated splenic arterioles (Figure S3E). Even in fully developed spleens, some *Mfge8*$^+$ cells remained associated with central arterioles (Figure S3F).

We then assessed the transcription of genes associated with FDC and/or LTβR activation (Huber et al., 2005) (Figures 2D and S3G). All FDC-deficient spleens had lower levels of *Mfge8*, *Cxcl13*, *Clusterin*, and *Igfbp3* ($p < 10^{-4}$ for each transcript) than WT spleens. In *Tnfr1*$^{-/-}$, *Rag1*$^{-/-}$, and μMT^D spleens the reduction was less pronounced than in *Lta*$^{-/-}$, *Ltb*$^{-/-}$, *Ltbr*$^{-/-}$, and *Rag2*$^{-/-}\gamma c^{-/-}$ mice, suggesting that FDC maturation was arrested at a later stage. *Cd21* expression was strongly reduced in B cell-deficient spleens (*Rag1*$^{-/-}$ and μMT^D, $p < 10^{-4}$), slightly diminished in *Lta*$^{-/-}$ (n.s.), *Ltb*$^{-/-}$ ($p < 0.01$) and *Ltbr*$^{-/-}$ spleens (n.s.), and remained unchanged in *Tnfr1*$^{-/-}$ spleens. The dearth of *Cd21* transcripts in mice lacking B cells but containing abundant preFDC confirmed that preFDC do not express *Cd21*, in accordance with the failure of Mfge8/CD21/35 stains to identify double-positive cells around the MS of WT mice (Figure 1C). Furthermore, no protein staining for CD21/35 could be observed in *Rag1*$^{-/-}$, μMT^D or *Rag2*$^{-/-}\gamma c^{-/-}$ spleens (data not shown). Hence within the FDC lineage *Cd21* transcription is restricted to fully mature FDC.

Expression of *Mfge8* in *Rag2*$^{-/-}\gamma c^{-/-}$ was much lower than in *Rag1*$^{-/-}$ mice (Figures 2A–2D). We suspected this to be caused by a further reduction in LTβR signaling. Indeed *Lta* mRNA was lower in *Rag2*$^{-/-}\gamma c^{-/-}$ spleens ($p < 0.05$, Figure 3A). Also, *Tnfa* transcripts were slightly reduced (n.s., Figure 3B). We then treated *Rag2*$^{-/-}\gamma c^{-/-}$ mice with an agonistic LTβR antibody (Rennert et al., 1998). Within 24 hr, splenic *Mfge8* was upregulated compared to isotype-treated mice (Figure 3C).

NK Cells Are Dispensable, but Lymphoid Tissue Inducer Cells Are Necessary for preFDC

A consequence of γc deficiency is the absence of NK cells. Because activated NK cells express LTαβ, we wondered whether they might induce *Mfge8*$^+$ preFDC (Ware et al., 1992). We therefore depleted NK cells from *Rag1*$^{-/-}$ mice using anti-NK1.1 antibodies (Strick-Marchand et al., 2008), and confirmed depletion by flow cytometry (isotype-treated mice 49 ± 8, anti-NK1.1-treated 0 ± 0% NK1.1$^+$DX5$^+$ NK cells; Figure S3H). We also observed a slight rise in DX5$^+$ single positive cells in NK cell depleted mice (control: 2.0 ± 0.4%, NK1.1 depleted: 7.5 ± 1.6%; Figure S3H). These cells could either be few remaining NK cells unable to bind NK1.1 antibodies due to competition with the NK1.1 antibody used in the treatment, or non-NK DX5$^+$ cells that have increased as a result of the treatment. *Mfge8* expression (qPCR and ISH) remained unaltered compared to isotype-treated mice (Figure 3D), indicating that NK cells are dispensable for *Mfge8* induction and no relevant source of LT.

Lymphoid tissue inducer (LTi) cells can also express LTαβ. Embryonic LTi are essential for the induction of various SLO, yet have no impact on splenic development (Cupedo et al., 2004; Eberl et al., 2004; Finke et al., 2002; Mebius et al., 1997; Zhang et al., 2003). Adult LTi cells were observed in spleens of WT, *Rag1*$^{-/-}$, and *Rag2*$^{-/-}$ mice (Kim et al., 2008; Takatori et al., 2009). However, although *Rag2*$^{-/-}\gamma c^{-/-}$ mice contain residual LTi cells, they are numerically reduced and express diminished levels of stimulatory molecules (Takatori et al., 2009).

Total LTi cell (B220$^-$CD3$^-$CD4$^+$Il7R$^+$) counts in *Rag2*$^{-/-}\gamma c^{-/-}$ were significantly lower than in *Rag1*$^{-/-}$ mice (Figure 3E) and LTi-specific CD30 ligand (*Cd30l*) mRNA was profoundly reduced (Figure 3F), suggesting an involvement of LTi cells in the generation of *Mfge8*$^+$ cells. We therefore crossed *Rorc(γt)*$^{-/-}$ mice, which lack LTi cells (Eberl et al., 2004), with *Rag1*$^{-/-}$ mice. Although *Rorc(γt)*$^{-/-}$ mice showed normal splenic organization and localization of mature *Mfge8*$^+$ FDC (Figure 3G), *Rag1*$^{-/-}$*Rorc(γt)*$^{-/-}$ spleens displayed strongly reduced *Mfge8* transcription and far fewer *Mfge8*$^+$ cells than *Rag1*$^{-/-}$ spleens (Figure 3H). No residual white pulp structures were found in *Rag1*$^{-/-}$*Rorc(γt)*$^{-/-}$ spleens. Therefore, in the absence of B cells, the interaction of LTi cells (rather than NK cells) with the splenic stroma triggers early steps of white pulp development including the generation of preFDC.

Splenic Mfge8$^+$ Cells Are Induced Perivascularly from PDGFRβ$^+$ Cells

To identify transient stages between perivascular *Mfge8* expressing cells and mature follicular FDC, we induced follicle development in *Rag2*$^{-/-}\gamma c^{-/-}$ mice by administering BM or splenocytes. We either used WT (data not shown) or *Mfge8*$^{-/-}$ BM (Figure 4A), or transferred WT splenocytes (data not shown; Kapasi et al., 1993). By transferring BM, the spleen was supplied continuously with physiologic numbers of lymphocytes, whereas the total splenocytes transfer was used to examine the behavior of perivascular preFDC responding specifically to mature lymphocytes. The use of *Mfge8*$^{-/-}$ BM ensured that induced Mfge8$^+$ cells were indeed host-derived. At day 3 after BM transfer, we observed an influx of B and T cells at sites of *Mfge8* expression. *Mfge8*$^+$ cells were further induced at the lymphocyte entry points (Figure 4A, top row). At day 13, many *Mfge8*$^+$ cells populated the perivascular areas and engaged in various stages of follicle formation (Figure 4A, bottom row). Transfer of WT BM

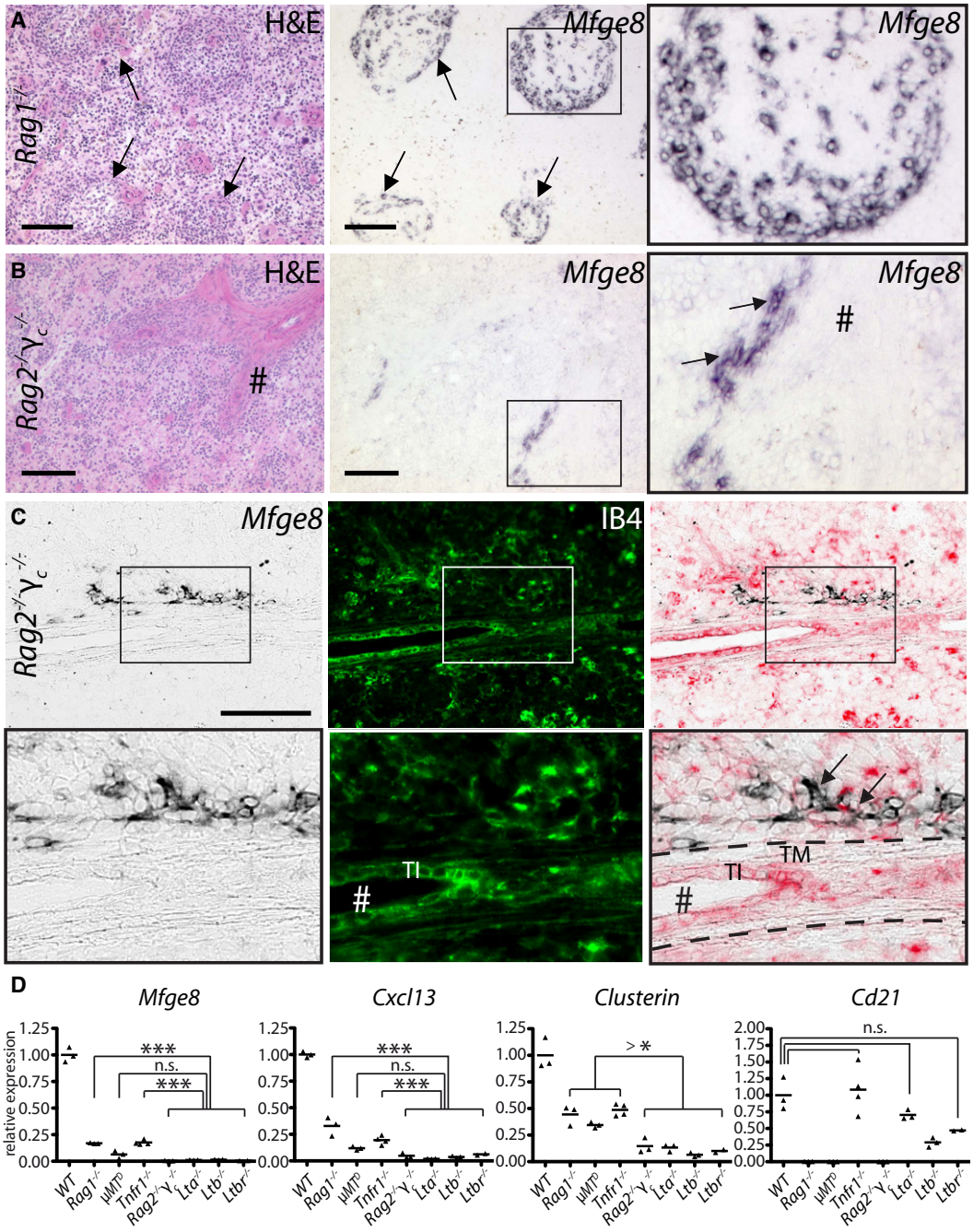

Figure 2. *Mfge8*$^{+}$ Cells in Mice Lacking Lymphocyte Subsets

(A and B) ISH for *Mfge8* on consecutive splenic cryosections of *Rag1*$^{-/-}$ (A) and *Rag2*$^{-/-}\gamma c^{-/-}$ mice (B). # (here and hereafter) indicates central arterioles, arrows: *Mfge8*$^{+}$ preFDC surrounding the residual white pulp in *Rag1*$^{-/-}$ spleens or adjacent to the vasculature in *Rag2*$^{-/-}\gamma c^{-/-}$ spleens.

(C) *Mfge8* ISH (left), isolectin B4 histochemistry (IB4, middle), and overlay (right; IB4 shown in red) of a *Rag2*$^{-/-}\gamma c^{-/-}$ spleen. TI, tunica intima; TM, tunica media.

(D) Relative abundance of *Mfge8*, *Cxcl13*, *Clusterin*, and *Cd21* transcripts in WT, *Tnfr1*$^{-/-}$, *Lta*$^{-/-}$, *Ltb*$^{-/-}$, *Ltbr*$^{-/-}$, *μMT*^{D}, *Rag1*$^{-/-}$, and *Rag2*$^{-/-}\gamma c^{-/-}$ spleens (qPCR, n = (2–4) × 3 technical replicas [here and thereafter in qPCR measurements]). Statistics (here and thereafter): unpaired t test; n.s., not significant; *p < 0.05; **p < 0.01; ***p < 0.001.

and splenocytes yielded identical results. Thus, we can conclude that mature lymphocytes, probably B cells, are sufficient to induce expansion of preFDC and differentiation into FDC.

To confirm these findings in normal splenic ontogeny, we assessed postnatal (P) development in WT mice. At day P0 and P1 no splenic *Mfge8*$^{+}$ cells were identified (data not shown).

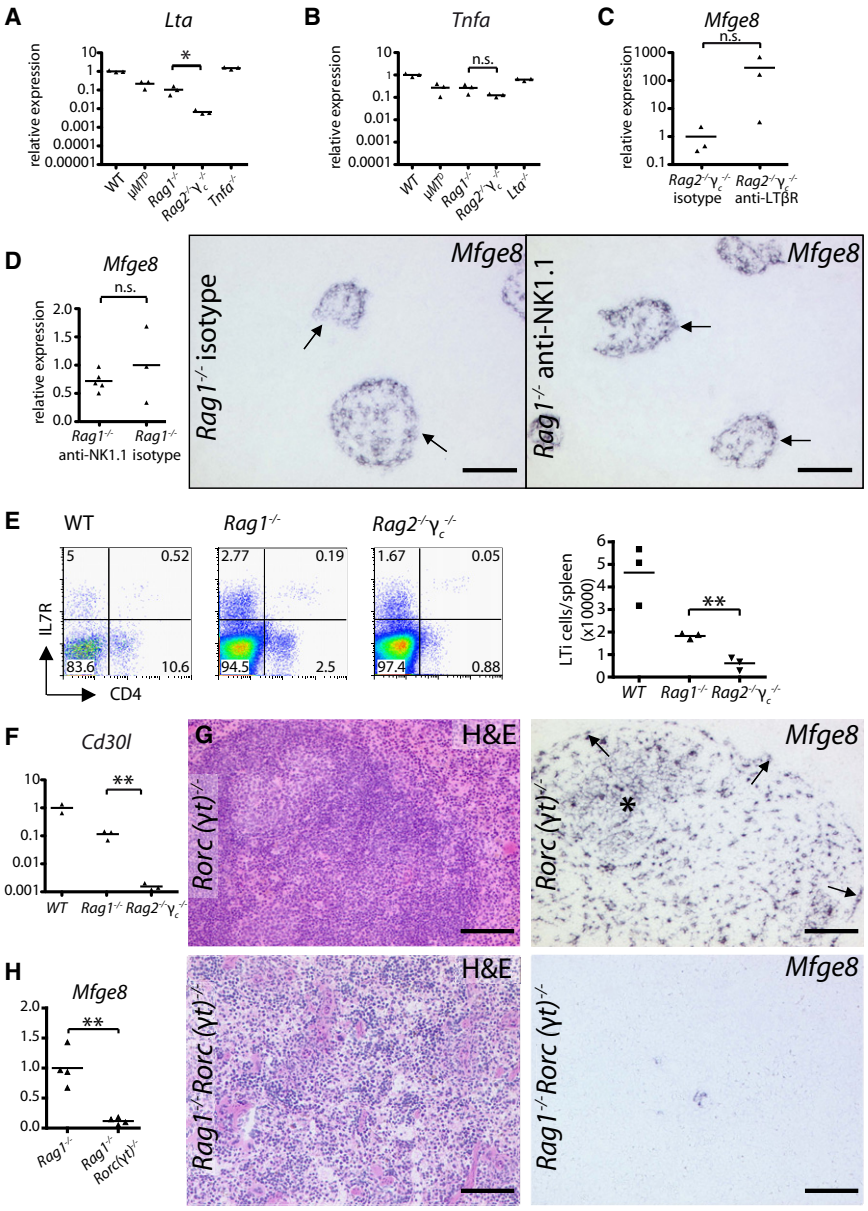

Figure 3. *Mfge8* Expression Is Driven by LTβR Activation, and Depends on LTi Cells

(A and B) *Lta* and *Tnfa* mRNA expression in μMT^{D}, $Rag1^{-/-}$, $Rag2^{-/-}\gamma c^{-/-}$, and $Tnfa^{-/-}$, or $Lta^{-/-}$ spleens compared to WT by qPCR (n = 3 × 3). $Rag2^{-/-}\gamma c^{-/-}$ had significantly reduced levels of *Lta* compared to $Rag1^{-/-}$.

(C) Induction of *Mfge8* expression in $Rag2^{-/-}\gamma c^{-/-}$ mice after treatment with agonistic anti-LTβR antibody compared to isotype control (n = 3 × 3).

(D) *Mfge8* expression in $Rag1^{-/-}$ spleens upon treatment with anti-NK1.1 or isotype-controlled antibody (n = (3–5) × 3), is not significantly changed in NK-depleted spleens. ISH for *Mfge8* on consecutive splenic sections of $Rag1^{-/-}$ mice treated with anti-NK1.1 antibody or isotype control. Arrows point to $Mfge8^{+}$ and residual white pulp structures (HE staining) remaining present in both treatment groups.

(E) Prevalence of $B220^{-}CD3^{-}$ (pre-gated) $CD4^{+}$ $IL7R^{+}$ LTi cells in WT, $Rag1^{-/-}$ and $Rag2^{-/-}\gamma c^{-/-}$ spleens (FACS; n = 3). $Rag2^{-/-}\gamma c^{-/-}$ showed significantly fewer LTi cells than $Rag1^{-/-}$.

(F) Relative expression of *Cd30l* in WT, $Rag1^{-/-}$, and $Rag2^{-/-}\gamma c^{-/-}$ spleens (n = (2–3) × 3). Compared to $Rag1^{-/-}$ *Cd30l* is significantly reduced in $Rag2^{-/-}\gamma c^{-/-}$ spleens.

(G) *Mfge8* ISH on $Rorc(\gamma t)^{-/-}$ spleens reveals FDC clusters and normal preFDC.

(H) Significant reduction of *Mfge8* in $Rag1^{-/-}$ $Rorc(\gamma t)^{-/-}$ compared to $Rag1^{-/-}$ spleens by quantitative PCR (n = 4 × 3). HE staining and ISH for *Mfge8* on $Rag1^{-/-}Rorc(\gamma t)^{-/-}$ splenic sections. See also Figure S3.

By P2, along with an influx of B and T lymphocytes, low *Mfge8* expression was detectable in situ and $Mfge8^{+}$ cells enclosed vascular structures (Figure S4A; Balogh et al., 2001). CD21/35 expression remained low during early postnatal stages, reflecting the influx of immature $CD21/35^{low}$ B cells (Loder et al., 1999). Stronger expression of *Mfge8* and CD21/35 was found at P10, when defined white pulp areas had been established (Figure S4B). Typical $CD21/35^{+}$ FDC networks as well as segregated B cell follicles and T cell zones were observed by P14 (Figure S4C).

These observations suggested a vessel-associated origin of FDC. Maintenance of blood vessels depends on mural cells residing in the outer vessel wall (Adams and Alitalo, 2007), which consist of pericytes directly contacting the vascular endothelium and vascular smooth muscle cells (vSMC) surrounding vessels. Although pericytes and vSMC differ in their morphological appearance and localization, they share the expression of platelet-derived growth factor receptor beta (PDGFRβ) and chondroitin sulfate proteoglycan 4 (NG2), vSMC furthermore express SMA (Adams and Alitalo, 2007; Armulik et al., 2011; Gaengel et al., 2009). Mfge8 is present on retinal pericytes, and appears to positively regulate PDGFRβ signaling (Motegi et al., 2011a, 2011b). Furthermore, T zone reticular cells (TRC) wrap blood vessels in a pericyte-like fashion in spleen and lymph nodes (Gretz et al., 1997; Link et al., 2007).

To test whether the earliest $Mfge8^{+}$ cells might be mural, we stained consecutive sections of $Rag2^{-/-}\gamma c^{-/-}$ spleens with PDGFRβ or hybridized them with the *Mfge8* riboprobe. Indeed, $Mfge8^{+}$ clusters colocalized with a fraction of the vascular $PDGFR\beta^{+}$ cells, suggesting that some mural cells had acquired FDC-like characteristics (Figure S4H). We then performed co-IF stains of mural cell markers with Mfge8 protein on WT splenic sections. Whereas mature FDC did not express any of these markers, preFDC of the MS colocalized with PDGFRβ, and SMA staining, but not NG2 (Figures 4B, S4D, and S4E)

and were positioned along IB4$^+$ MS vascular endothelium (Figure S4F).

We then asked whether mature FDC express low levels of PDGFRβ undetectable by IF. By flow cytometry, FDC are mostly restricted to a stromal (CD45$^-$) CD31$^-$GP38$^-$ cell population (Link et al., 2007). To positively identify functional FDC within the latter population, we used in vivo trapping of intravenously administered phycoerythrin immune complexes (IC-PE; Figure S4G; Phan et al., 2007). We found no expression of PDGFRβ on stromal IC-PE$^+$ cells within the CD31$^-$GP38$^-$ fraction (Figures 4C and S4I). However, PDGFRβ was present on cells within the TRC (CD31$^-$GP38$^+$) population (Figures 4C and S4I) (Link et al., 2007). Hence mature FDC do not express PDGFRβ.

If FDC derive from perivascular cells, they may transiently express mural markers during histogenesis. We therefore analyzed *Pdgfrb*-expressing cells in spleens of *Pdgfrb*-Cre$^+$ mice crossed to a Cre-inducible fluorescent reporter (CAG-tdTomato [Ai14]; Madisen et al., 2010) or to a *lac*Z reporter (R26R) (Foo et al., 2006). tdTomato and LacZ were primarily observed in highly vascularized areas of the spleen (red pulp, marginal sinus, and central arteriole) (Figures 4D and S4K). Crucially, both reporter genes were present within the white pulp, particularly in areas containing mature FDC. Confocal imaging showed cellular colocalization of tdTomato and Mfge8$^+$ FDC (Figure 4, > 80% of Mfge8$^+$ FDC were tdTomato$^+$). No tdTomato signal or LacZ staining was seen in *Pdgfrb*-Cre$^-$ littermates (Figures S4J and S4K).

We then conditionally ablated the mural cell lineage from mature spleens. For this purpose we interbred Pdgfrb-Cre mice with iDTR mice carrying a diphtheria toxin (DT) receptor gene preceded by a *lox*P-flanked stop cassette (Buch et al., 2005). Cre expression allows selective depletion of DTR-expressing cells upon DT treatment. Indeed, FDC networks were massively reduced after ablation of PDGFRβ-derived cells by a 3-day drug treatment (Figure 5A, second row). The depletion had dire consequences on the overall organization of the B cell follicles as well: only remnants could be observed after DT treatment. GP38$^+$ follicular reticular cells were also affected, though to a lesser degree (Figure S5B). Pdgfrb-Cre$^+$iDTR$^+$ mice that had not been exposed to DT, and DT-treated Cre$^-$iDTR$^+$ littermates, maintained a normal splenic microarchitecture (Figure 5A, top row).

FDC Precursors Are of Stromal Origin, Sessile, and Not Restricted to Lymphoid Organs

If FDC originate from ubiquitous PDGFRβ$^+$ perivascular cells, local precursors from any vascularized organ should be able to differentiate into FDC. We investigated this question by studying ectopic TLT at sites normally devoid of FDC (liver, kidney, and white adipose tissue).

Activation of LTβR is the main driver of FDC differentiation. To stimulate maturation of precursors in nonlymphoid organs, we subjected WT mice to a treatment with agonistic anti-LTβR antibodies and compared the relative expression of *Mfge8*, *Cxcl13*, *Vcam1*, *Icam1*, *Madcam1*, and *Pdgfrb* to isotype-treated mice (Figure 5B). In agonist-treated livers, *Mfge8*, *Cxcl13*, *Vcam1*, and *Icam1* were upregulated, whereas *Pdgfrb* was reduced. *Madcam1* remained below the detection limit in either treatment group. In kidneys and fat tissue *Mfge8*, *Cxcl13*, *Vcam1*, *Icam1*, and *Madcam1* were also found to be upregulated.

We then directly tested the hypothesis that FDC precursors exist in nonlymphoid organs. Kidneys of *RIP-Lta* transgenic mice develop follicular nephritis due to renal LT overexpression (Picarella et al., 1992). We transiently depleted *RIP-Lta* mice of FDC by administration of LTβR-Ig or isotype control (n = 4–5 for each group). Mice were then lethally irradiated to deplete any kidney-resident hematopoietic cells; one kidney from each mouse was analyzed histologically to confirm FDC depletion, and the second kidney was transplanted into prion protein deficient mice (*Prnp*$^{-/-}$) (Büeler et al., 1992; Tian et al., 2010) (Figure S5D). The reappearance of FDC in transplanted kidneys was studied using PrP, which is highly expressed by FDC, as a histogenetic marker of donor-derived cells. LTβR-Ig treatment eliminated FDC-M1$^+$CD21/35$^+$PrP$^+$ FDC before transplantation, and lymphocytic infiltrates were strongly reduced in number and size (Figure S5C and data not shown). As a further control, we transplanted kidneys from WT mice that had been treated with LTβR-Ig or the isotype control. No TLT or other pathologic alterations were found by histology in these WT kidneys before transplantation (data not shown). At 12 weeks posttransplantation, kidneys were analyzed for the presence of FDC and TLT (Figures 5C and S5D). Transplanted RIP-Lta kidneys had regained FDC networks that were mostly Mfge8$^+$PrP$^+$. Some Mfge8$^+$ cells were found to be PrP$^-$, but costaining for CD68 identified them as recipient-derived macrophages (Kranich et al., 2008). Therefore autochthonous FDC precursors exist in nonlymphoid organs such as the kidney.

These and previous results suggest that the FDC precursor is a PDGFRβ$^+$ cell present in the vasculature of lymphoid and nonlymphoid tissues. We tested this prediction by analyzing PDGFRβ$^+$ cells from the white adipose tissue (WAT) of the perigonadal fat pad, whose vascular components can be easily isolated (Tang et al., 2008). Whereas the mesenteric fat and the milky spots can contain lymphocytic clusters (Moro et al., 2010), we did not detect lymphocytes in the perigonadal fat pad (Figure S6A). In particular, flow cytometry showed that CD23^{high}CD21/35^{low} follicular B cells, which are essential for FDC maturation, were absent (Figure S6B), whereas most hematopoietic cells were macrophages (CD45$^+$CD11b$^+$, Figure S6C).

We next dissected stromal-vascular (SV) compartment of perigonadal fat and sorted PDGFRβ$^+$ cells by FACS (Figure S6D; purity in this and subsequent sorts: 94%–98.9%). We confirmed the identity of the isolated cells with qPCR (*Pdgfrb* and *Ng2*, Figure 6A) and excluded relevant levels of contamination with fat (*Perilipin*, *Plin1*) or hematopoietic cells (*Cd45*) (Figures S6E and S6F). The expression of FDC-characteristic mRNA was assessed in isolated PDGFRβ$^+$ cells and compared to that of spleens (Figure 6A). Some transcripts were reduced (*Mfge8* [37%], *Cxcl13* [21%], *Vcam1* [64%], *Igfbp3* [96%]), whereas others were highly abundant (*Icam1* [235%], *Enpp2* [240%], *Periostin* [120-fold] [*Postn*], and *stromal cell-derived factor 1* [254%] *Sdf1*). In contrast, *Clusterin* (4%), *Madcam1* (2%), *Bp-3* (0.3%), *Cd21* (0.6%), and *Fcgr2b* (0.6%) were downregulated. Thus isolated perivascular PDGFRβ$^+$ cells were phenotypically similar to preFDC; the low abundance of *Cd21* and *Fcgr2b* transcripts suggests that these are mainly involved in later stages of

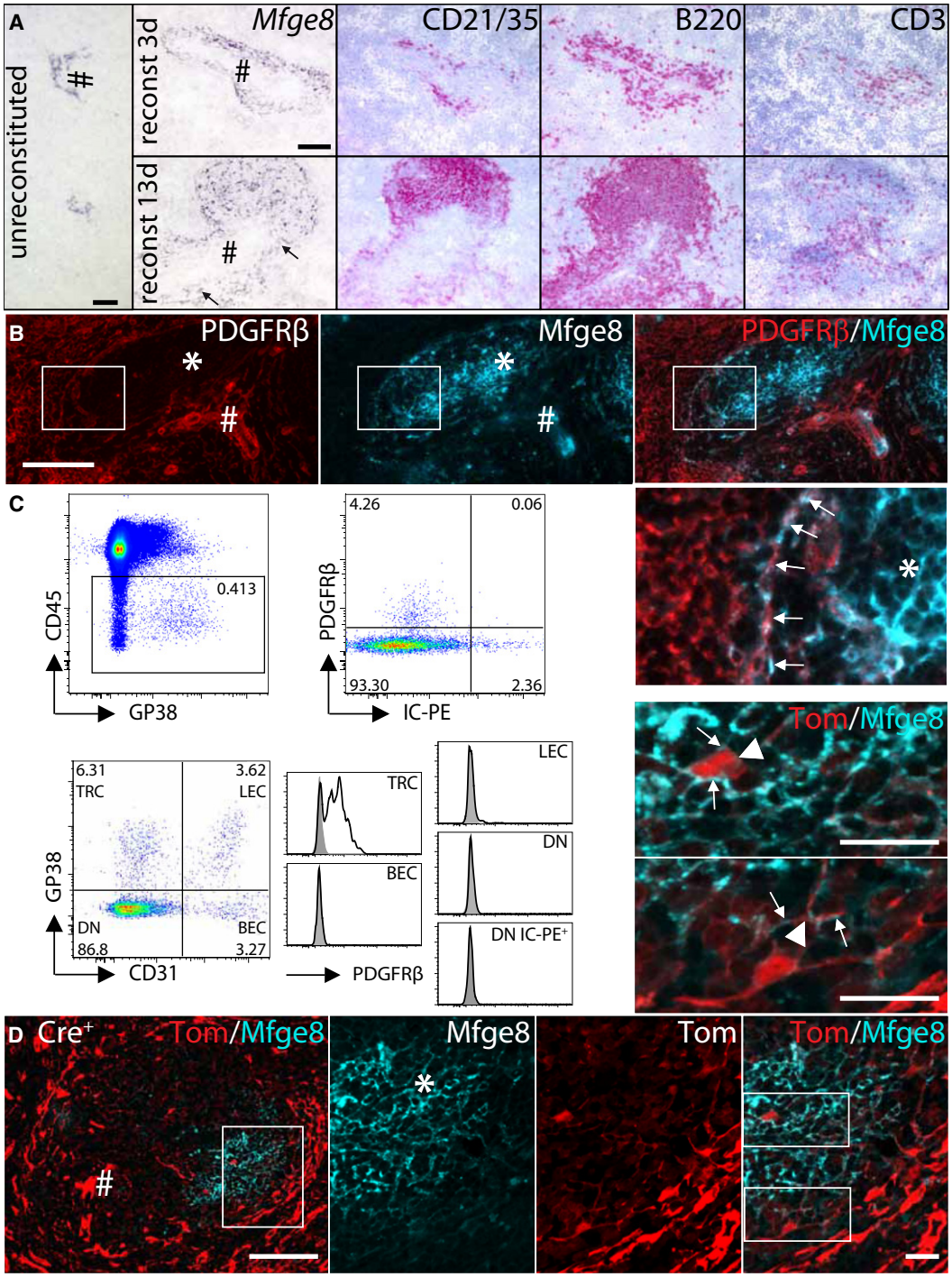

Figure 4. Perivascular Induction of FDC Development

(A) *Rag2*$^{-/-}\gamma c^{-/-}$ mice were reconstituted with *Mfge8*$^{-/-}$ BM and analyzed at 3–13 days (d3–13) after transfer. *Mfge8* ISH on unreconstituted *Rag2*$^{-/-}\gamma c^{-/-}$ spleen (left), d3 (upper row), and d13 (lower row) postreconstitution. Consecutive sections stained for B cells (CD21/35 and B220) and T cells (CD3). Arrows: *Mfge8*$^{+}$ cells.

(B) Co-IF of PDGFRβ and Mfge8 on preFDC, but not on mature FDC of WT spleens.

(C) Flow cytometric analysis for PDGFRβ on stromal cells isolated from the inguinal lymph nodes (LN) of mice that had received IC-PE. Within the stromal fraction (CD45^{-}, upper row left) PDGFRβ expression was restricted to the IC-PE negative fraction (upper row right). Expression of PDGFRβ was then determined within the four stromal (CD45^{-}) subpopulations by staining with CD31 and GP38 (lower row left). T zone reticular cells (TRC, CD31^{-}GP38^{+}), lymphatic endothelial cells (LEC, CD31^{+}GP38^{+}), blood endothelial cells (BEC, CD31^{+}GP38^{-}), double-negative (DN) cells (CD31^{-}GP38^{-}) cells containing FDC (DN IC-PE^{+}). Only TRC showed increased expression of PDGFRβ (unshaded) over isotype control stained sample (shaded).

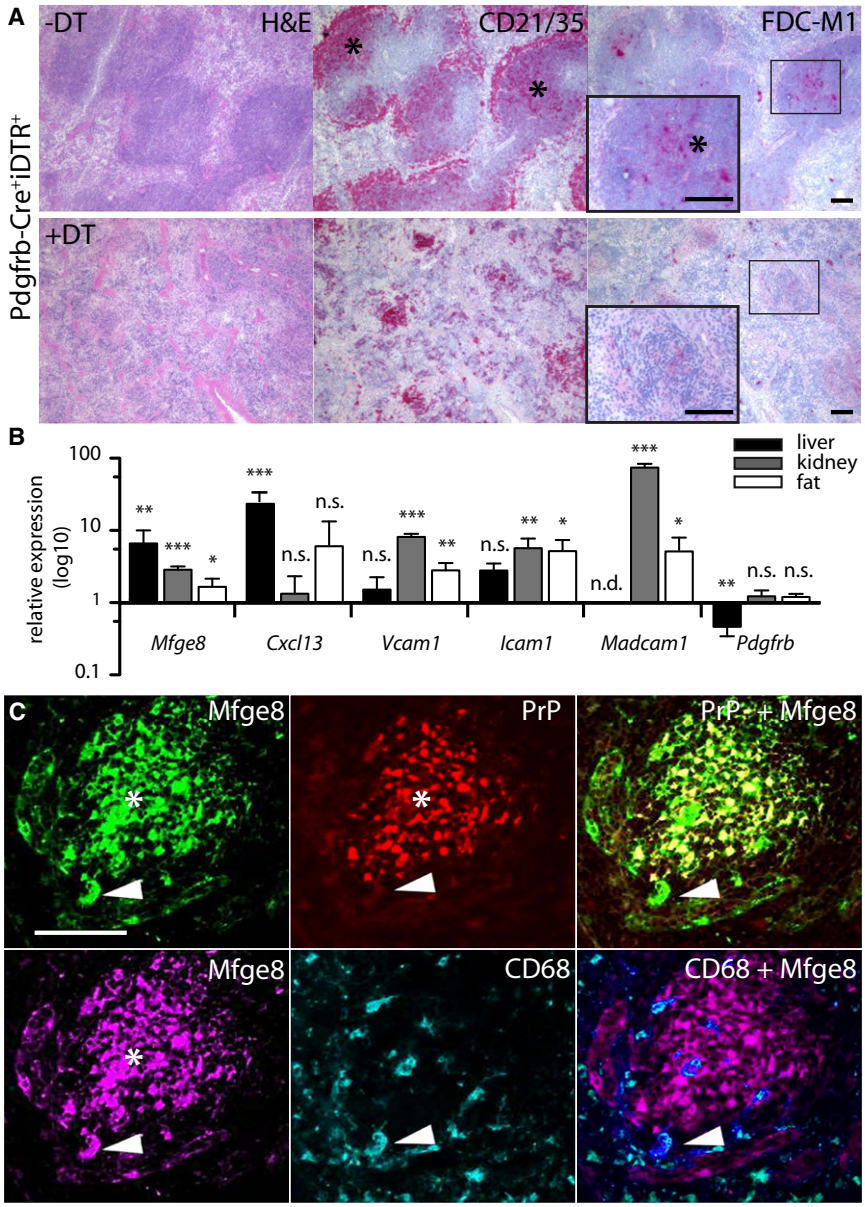

Figure 5. FDC Are Derived from PDGFRβ⁺ Precursors and Are Present in Nonlymphoid Organs

(A) Targeted ablation of *Pdgfrb*-expressing cells. Pdgfrb-Cre⁺iDTR⁺ mice were treated for 3d with DT (lower row) and compared to PBS-treated littermates (upper row). Consecutive splenic sections were stained with H&E, CD21/35, and FDC-M1. FDC-M1 staining is absent and CD21/35 positivity drastically reduced in the vestigial follicular structures of DT-treated mice.

(B) WT mice were treated for 24 hr with agonistic anti-LTβR i.v. (liver; n = 5 × 3) or i.p. (kidney and fat; n = 4 × 3) and the relative expression of FDC-related transcripts was analyzed by qPCR in agonist-treated versus isotype-treated mice. Error bar, SEM.

(C) *RIP-Lta* kidneys were depleted of FDC using LTβR-Ig before transplantation into *Prnp*$^{-/-}$ mice (n = 4). Twelve weeks after transplantation, IF analysis was performed on kidney cryosections. Mfge8 (green or magenta) detects FDC networks and tingible body macrophages, PrP (red) stains donor-derived FDC networks and CD68 (cyan) detects tingible body macrophages. Most Mfge8⁺ cells are PrP⁺. Arrowhead: Mfge8⁺/PrP⁻CD68⁺ cell reflecting *Prnp*$^{-/-}$ derived tingible body macrophages. For better visualization a violet pseudocolor was used in the overlay of CD68⁺ and Mfge8⁺ cells (middle lower panel).

See also Figure S5.

FDC development, in agreement with our in vivo observations (Figures 1C, 2D, and S1C).

Differentiation of FDC requires activation of TNFR1 and LTβR; both were highly expressed in isolated fat PDGFRβ⁺ SV cells (Figure 6A). We then cultured these cells for 24 hr in the presence of agonistic anti-LTβR antibody and TNF, and analyzed the induction of FDC markers by qPCR (Figure 6B; Katakai et al., 2008). We found upregulation of *Vcam1*, *Icam1*, *Madcam1*, and *Enpp2* over isotype-treated cells, concomitant with loss of *Pdgfrb* expression. *Mfge8* and *Igfbp3* were not significantly changed (Figure 6B). We did not detect *Cd21* and *Fcgr2b*, possibly because the in vitro conditions did not supply all signals needed for terminal FDC differentiation.

We then sorted PDGFRβ⁺ cells also from *Rag2*$^{-/-}\gamma c^{-/-}$ perigonadal WAT, and determined FDC-related transcripts (Figure S6G). *Mfge8* (113%), *Cd21* (82%), and *Tnfr1* (87%) were expressed at similar levels as in WT PDGFRβ⁺ cells; *Icam1* (77%) and *Vcam1* (47%) were reduced, whereas *Pdgfrb* (160%) and *Ltbr* (146%) were slightly upregulated. Thus WT PDGFRβ⁺ cells did not show a more mature differentiation pattern for FDC. Because *Rag2*$^{-/-}\gamma c^{-/-}$ mice do not contain mature FDC, this finding provides further evidence that perigonadal fat does not contain FDC (Figures S6A–S6C).

To test whether fat PDGFRβ⁺ SV cells were indeed precursors of mature FDC, purified cells were absorbed into a collagen sponge and transplanted into the renal subcapsular space of FDC-deficient hosts (*Ltbr*$^{-/-}$). Mice were immunized and

(D) IF staining for Mfge8⁺ FDC on splenic section from *Pdgfrb-Cre*⁺ Ai14⁺ mice showing strong expression of the reporter protein tdTomato within the vascular components (left, scale bar 20 μm). Higher magnification (indicated by box) on the FDC area (middle (from left to right: Mfge8, tdTomato, overlay, scale bar 20 μm), showing expression of reporter on FDC cell body and dendrites (higher magnification).

See also Figure S4.

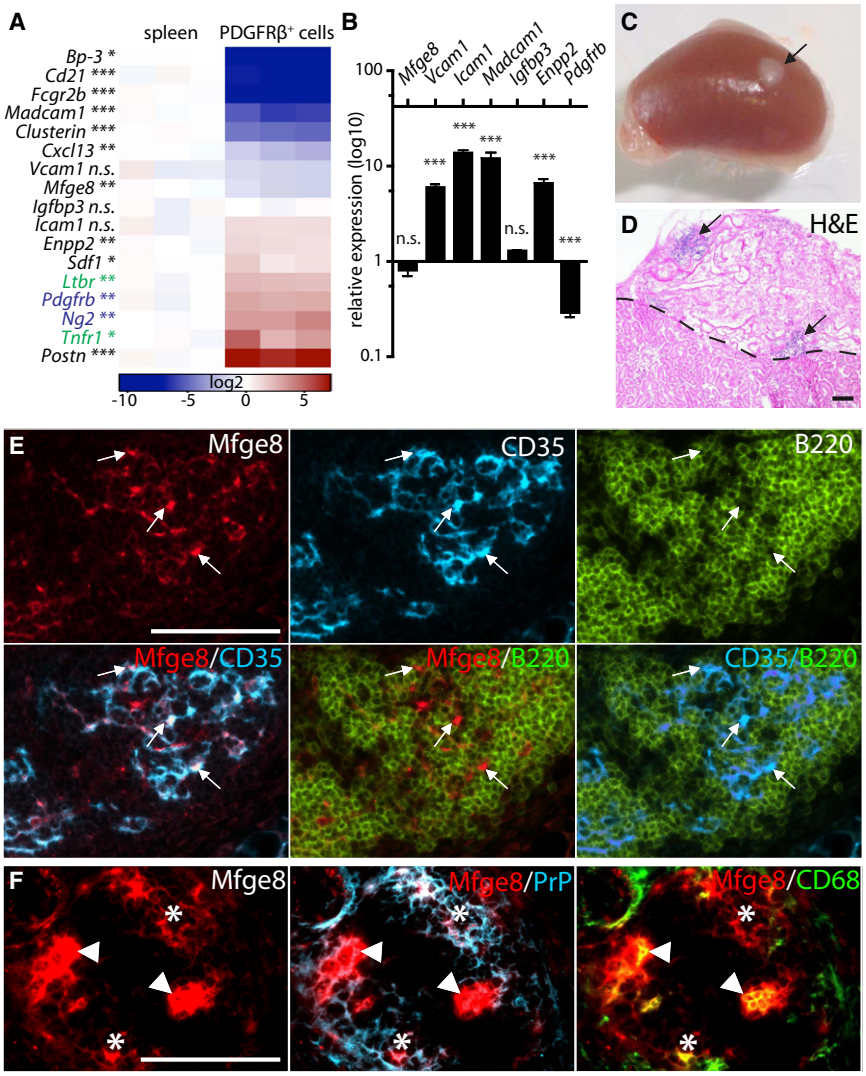

Figure 6. PDGFRβ⁺ Cells Are FDC Precursors

(A) FDC markers (black), FDC receptors (green), and mural cell marker (blue) were assessed by qPCR in PDGFRβ⁺ cells FACS-sorted from perigonadal WAT. Measurements are presented in a $\log_2$ scale (blue, downregulated; red, upregulated; white, no change in expression). Columns indicate individual samples. Each data point reflects the median expression of a particular gene normalized to its mean expression in WT spleens (n = 3).

(B) PDGFRβ⁺ cells were FACS-sorted from perigonadal WAT and stimulated for 24 hr with agonistic anti-LTβR antibody and TNF (n = 3 × 3). RT-PCR was performed for *Mfge8*, *Icam1*, *Vcam1*, *Madcam1*, *Enpp2*, *Igfbp3*, and *Pdgfrb*. Figure shows relative expression compared to isotype-treated PDGFRβ⁺ cells. Error bar, SEM.

(C–F) Renal subcapsular transplantation of PDGFRβ⁺ cells. Isolated cells were absorbed into a collagen sponge and transplanted into *Ltbr*$^{-/-}$ recipients (n = 4). Mice were immunized and boosted i.v. and analyzed 4 weeks after the transplantation (C, arrow points to the transplant). (D) Section through the transplanted collagen sponge and kidney stained with H&E. Arrows point to lymphocytic infiltrates within the sponge. Dashed line marks the border between transplant and kidney. Transplanted PDGFRβ sponge contains FDC (Mfge8 and CD35) and B cells (B220) (E) and FDC (Mfge8 and PrP) and tingible body macrophages (TBM, Mfge8, and CD68 arrowheads) (F) as determined by Co-IF.

See also Figure S6.

boosted intravenously to stimulate the differentiation of FDC. Four weeks after surgery, transplants exhibited lymphocytic foci (Figures 6C and 6D) containing B220⁺CD21/35⁺ B and CD3⁺ T lymphocytes as well as putative CD21/35⁺ and FDC-M1⁺ FDC (Figure S6H, and data not shown). Co-IF identified B220⁺ B cell lymphoid follicles with CD35⁺Mfge8⁺ FDC networks (Figure 6E). Mfge8⁺ FDC also expressed FcγRIIβ (Supp. 6I) and PrP (Figure 6F), and CD68⁺Mfge8⁺ tingible body macrophages were detected within the lymphoid aggregates typical of active GC (Figure 6F). Aggregate formation appeared to be modulated by the immune status of recipient mice (Table S1), with positive sponges typically harboring ≥10 conspicuous lymphoid foci; sponges containing no PDGFRβ cells never developed such aggregates or FDC (Figure S6J). To deploy an additional genetic marker distinguishing between donor and host cells, we also transplanted PDGFRβ⁺ cells into *Cd21*/35$^{-/-}$ hosts and injected IC-PE to test the functionality of generated FDC. Again, we had generated host-derived CD21/35⁺ FDC clusters capable of capturing IC in vivo (Figure S6K and Table S1).

DISCUSSION

FDC can arise almost anywhere during chronic inflammations triggered, for example, by viral infections and autoimmunity. This implies that the putative FDC precursor cell may be either ubiquitous and sessile (Bofill et al., 2000; Lee and Choe, 2003), or it may possess considerable motility (Kapasi et al., 1998). We report that (1) the earliest expression of FDC markers in spleens occurs perivascularly; (2) mature FDC derive from progenitors transcribing *Pdgfrb*, a gene associated with mural cells; (3) mature FDC can be conditionally ablated in vivo by removing PDGFRβ⁺-derived cells; (4) precursors of FDC are present in nonlymphoid organs; (5) isolated PDGFRβ⁺ cells from nonlymphoid vascular stroma express FDC-associated genes; and (6) isolated PDGFRβ⁺ vascular cells differentiate into FDC-like cells in the presence of factors crucial for FDC differentiation and maintenance in vitro and develop into mature B cell-recruiting and IC-trapping FDC in vivo. We therefore posit that FDC are derived from mural cells expressing *Pdgfrb* and *Mfge8*.

These findings suggest a hierarchy of discrete steps in FDC development (Figure 7). The earliest PDGFRβ⁺ cells expressing *Mfge8*/*Cxcl13* are found at perivascular sites in mice lacking all white pulp structures (*Rag2*$^{-/-}\gamma c^{-/-}$) as well as in developing

	perivascular preFDC	marginal sinus preFDC	mature FDC
mural markers			
PDGFRβ	+++	+	-
NG2	+++	-	-
FDC-associated markers			
SDF1	++	n.d.	-
VCAM1	+	+	++
ICAM1	++	+	++
MAdCAM1	+/-	+	+
Mfge8	+	+	++
CXCL13	+	+	++
E-NPP2	++	+	++
IGFBP3	+	+	+
Periostin	+++	n.d.	+
Clusterin	+/-	+	+
BP-3	-	+	+
FcγRIIβ	-	+/-	+
CD21/35	-	-	+
TNFR1	+++	+	+
LTβR	+++	+	+
differentiation signals			
LTi cells, B cells		$LT\alpha\beta_2$	
B cells			$LT\alpha\beta_2$, TNF

Figure 7. Model of FDC Maturation

In the spleen, a subpopulation of vascular/perivascular PDGFRβ$^+$ cells progress to the preFDC stage expressing FDC markers. Signals inducing the upregulation of these markers remain to be defined. In response to LTβR activation and probably other signals provided by LTi cells, perivascular cells expand, populate the early white pulp structures and the marginal sinus. Marginal sinus preFDC have reduced levels of mural cell markers and upregulate the FDC markers Clusterin and BP-3. In presence of B cells and through activation of TNFR1 signaling, preFDC further mature into functional FDC, acquiring the ability to trap antibody and immune complexes via the expression of CD21/35 and FcγRIIβ. Perivascular preFDC: expression of markers was determined in situ by RNA hybridization (*Mfge8* and *Cxcl13*), immunohistochemistry (IHC) and IF or by relative RNA expression levels in isolated adipose PDGFRβ$^+$ cells and in spleens from *Rag2*$^{-/-}\gamma c^{-/-}$ and *LT*-deficient mice compared to wild-type (WT) spleen levels. (–) Expression is not detectable or below 0.6% of WT spleen; (+/–) expression 1%–4% of WT spleen; (+) 20%–100% of WT spleen; (++) 100%–250% of WT spleen; (+++) more than 500% of WT spleen. Marginal sinus and white pulp preFDC: (+) and (–) according to IF and ISH stains in WT, *Rag1*$^{-/-}$, and *TNF*-deficient mice or by relative RNA expression determined in *Rag1*$^{-/-}$, *μMT*^{D}, and *TNF*-deficient mice. (+/–) very low expression detected by IF; n.d., not determined. Mature FDC: marker expression according to quantitative expression data, ISH and IF performed on spleens from WT mice and according to previous reports.

neonatal spleens. These cells appear to represent FDC precursors, and we therefore termed them "preFDC." Much evidence suggests that preFDC are the immediate precursors to mature FDC: they express many typical FDC markers, are radioresistant, and behave as stromal residents in bone marrow transfer experiments. Conversely, preFDC are not ultrastructurally recognizable as FDC, do not express complement receptors, and only minute amounts of Fcγ receptors. Hence they are less specialized than mature FDC. Finally, preFDC express chemokines and adhesion molecules, suggesting relevance in the splenic microarchitecture.

In *Rag2*$^{-/-}\gamma c^{-/-}$ mice only few preFDC showed enhanced *Mfge8* and *Cxcl13* expression, suggesting that local stimuli trigger a phenotypic switch in select cells. *Rag2*$^{-/-}\gamma c^{-/-}$ mice contain functionally handicapped LTi cells located in perivascular areas; hence signals transmitted by residual LTi at vascular hotspots may suffice for PDGFRβ$^+$ mural cells to differentiate. Although LTβR signaling is necessary for SLO development, early *Mfge8* expression was LTβR-independent, suggesting the existence of additional LTi-dependent clues at this step of FDC ontogenesis. FDC precursors were postulated in the marginal sinus of TNFR1$^{-/-}$ and SCID mice (Pasparakis et al., 2000; Wilke et al., 2010) and final FDC maturation requires not only LTi cells but also B cells (Fu et al., 1998; Tumanov et al., 2004). Thus, even though LTi cells share with B cells the expression of most TNF ligands, such as LTαβ and TNF (Kim et al., 2006), the factors provided by LTi cells are insufficient for terminal FDC differentiation. Perhaps the signals supplied by LTi are quantitatively insufficient, or B cells deliver additional factors crucial for conversion of marginal sinus preFDC into mature FDC (Tumanov et al., 2004).

The above mechanisms may also apply to the generation of ectopic follicles, with mural cells generating FDC at any vascularized site. Innate immune reactions by local cells may induce inflammation at the endothelium allowing extravasation of lymphocytes, which, in turn, provide LTαβ and lead to the upregulation of Mfge8/CXCL13 on perivascular cells (Aloisi and Pujol-Borrell, 2006; Ludewig et al., 1998; Mebius, 2003). The latter may differentiate into FDC and provide the scaffold for developing follicular structures. Lymphocyte recruitment by transplanted stromal-vascular PDGFRβ$^+$ cells may be analogous to the generation of TLT, with donor-derived LTβR$^+$ FDC precursors cooperating with recipient-derived LTαβ$^+$ hematopoietic cells.

The finding that perivascular PDGFRβ$^+$ cells in nonlymphoid organs have FDC-like properties, and become mature FDC in vivo when exposed to the appropriate environment, implies that FDC generated de novo in tertiary lymphoid organs have arisen from these progenitor cells. The precise definition of the steps by which PDGFRβ$^+$ preFDC differentiate into FDC may

help understanding the pathogenesis of autoimmune and non-autoimmune chronic inflammations, the generation of nonlymphoid-organ-associated FDC sarcomas or infectious diseases such as AIDS and prion diseases.

EXPERIMENTAL PROCEDURES

Mice

Mice used are listed in the Extended Experimental Procedures. Animals were maintained under specific pathogen-free conditions. All experiments were in accordance with Swiss federal legislation and had been approved by the Cantonal Veterinary Authority of the Canton of Zurich.

Kidney Transplantation

RIP-Lta and WT mice were treated with 100 μg LTβR-Ig or isotype human-IgG weekly for 8 weeks, irradiated and isolated kidneys transplanted into $Prnp^{-/-}$ recipients (see Extended Experimental Procedures). Mice were sacrificed 12 weeks posttransplantation.

Bone Marrow Reconstitutions

For reconstitution of 6- to 8-week-old $Rag2^{-/-}\gamma c^{-/-}$ mice received $2x10^7$ donor bone marrow (BM) cells intravenously (i.v.) without previous irradiation, mice were sacrificed and organs taken at indicated time points.

Antibody Treatment

To block LTβR signaling mice (8–12 weeks) were treated with 100 μg mITβR-mIgG1 (Biogen) or isotype control (MOPC 21, Biogen) i.p. weekly for 4 weeks. For agonistic LTβR treatment 50 μg of anti-LTβR antibody (AC.H6, Biogen) or hamster IgG (Ha4/8-3.1, Biogen) were injected i.v. and mice sacrificed after 24 hr. Depletion of NK cells was performed using 100 μg anti-mouse NK1.1 (PK126, BD biosciences) or mouse IgG2a,κ (G155–178, BD biosciences) as isotype control injected i.v. weekly for 3 weeks.

In Vivo Immune Complex Trapping

Adapted from (Phan et al., 2007): 2 mg anti-phycoerythrin (PE) antibodies (Rocklands) were applied intraperitoneally (i.p.). Twelve hours later, mice were injected with PE (Invitrogen), 20 μg of i.p to target kidneys or subcutaneously (s.c.) into the flank with 10 μg to target inguinal lymph nodes and sacrificed 3–4 days later.

Depletion of Pdgfrb-Expressing Cells by Diphtheria Toxin Treatment

Eight- to 12-week-old PDGFRb-Cre^+ $iDTR^+$, PDGFRb-Cre^-, $iDTR^+$ male mice were treated for 3 days with 200 ng/day DT (Sigma) in PBS or PBS control i.p.

Immunohistochemical and Immunofluorescent Analysis

Cryosections were stained with hematoxylin/eosin (H&E) or primary antibodies and detection was performed using respective AP-coupled secondary and tertiary antibodies, Fast Red staining kit (Sigma) or on the Leica Bond-III IHC stainer. Tissues of mice expressing fluorescent protein reporters were pretreated before IF staining (Madisen et al., 2010). For IF splenic cryosections were stained (antibodies in Supplemental Information) and analyzed by fluorescence microscopy (BX61, Olympus) or CLSM Leica SP5, image processing software: Photoshop and Imaris - Multicolor and 4D Image Processing and Analysis (Bitplane).

β-Galactosidase Histochemistry

See also Extended Experimental Procedures. Sections were stained in FeKCN(II)/(III) solution containing X-Gal (Promega).

In Situ RNA Hybridization

See also Extended Experimental Procedures. Sections were incubated with DIG-labeled RNA probe in hybridization buffer. For detection an alkaline-phosphatase conjugated anti-DIG-antibody was used (Roche). For stainings with isolectin B4 (IB4), sections were incubated with biotinylated IB4 (Griffonia simplicifolia, Invitrogen) and avidin-FITC (BD biosciences) after the hybridization.

Isolation of Perigonadal White Adipose Stromal-Vascular Cell Fraction

Isolation of perivascular stromal cells was done as previously described (Tang et al., 2008). Briefly, perigonadal white adipose depots were minced into pieces and tissue digested in stromal cell isolation buffer (DMEM containing 2% fetal calf serum [FCS]) containing 1 mg/ml collagenase D (Roche) at 37°C. The suspension was passed through a 210 μm nylon and the adipocyte layer removed by aspiration and sorted by FACS (see FACS) to obtain a pure population of PDGFRβ$^+$ SV cells.

Isolation of Stromal Cells from Inguinal Lymph Nodes

Protocol adapted from (Link et al., 2007), mice with or without previous in vivo IC trapping were used. Details in Extended Experimental Procedures. LN were digested using collagenase IV, DNase I, and collagenase D. Cells were filtered through a 40 μm cell strainer and blocked 2% FCS, 2% mouse serum and anti-CD16/32 antibody (2.4G2), stained and subjected to FACS analysis (see FACS).

FACS

Single cell suspensions were made in PBS buffer containing 2% FCS, red blood cells lysis was performed in lysis buffer (eBioscience), cells were filtered through a 40 μm cell strainer. Fc-receptors were blocked with anti-CD16/32 antibody (2.4G2) and subsequently stained with antibodies (list in Extended Experimental Procedures). Cells were sorted by FACS Aria or analyzed by FACSCalibur or FACS Canto II flow cytometer (BD biosciences) and FlowJo software (Tree Star, Inc., USA).

PDGFRβ$^+$ SV cell culture

PDGFRβ$^+$ positively sorted adipose SV cells were maintained in DMEM (Invitrogen) with 10% FCS, 100 units/ml penicillin, and 100 μg/ml streptomycin. Cells were cultured for 24 hr with 100 ng/ml agonistic LTβR (AC.H6, Biogen) or hamster IgG (Ha4/8-3.1, Biogen) and 5 ng/ml mTNF (R&D Systems) and RNA was isolated by Trizol extraction.

Subcapsular Renal Transplantation of PDGFRβ^{2+} Stromal-Vascular Cells

Three hundred thousand to 500,000 FACS-sorted PDGFRβ$^+$ cells were absorbed into a collagen sponge (CS-35; KOKEN) of approximately 1 mm^3 size (Suematsu and Watanabe, 2004). The sponge was transplanted subcapsularly into the kidney. Mice were immunized 1 week after surgery with 2×10^8 sheep red blood cells (sRBC, ACILA AG), boosted after 15 days with 1×10^8 sRBC, and sacrificed 5 days later.

Quantitative RT-PCR

Total RNA from cells or livers, spleens, kidneys, fat or PDGFRβ$^+$ SV cells were isolated using Trizol (Invitrogen) and chloroform extraction. One microgram of RNA was used to generate cDNA using a QuantiTect Reverse Transcription Kit (QIAGEN). Quantitative real-time PCR was performed using SYBR Green PCR Master Mix (QIAGEN AG, Switzerland) on a 7900HT Fast Real-Time PCR System (Applied Biosystems) using default cycling conditions. Expression levels were normalized using *Gapdh*. Primer sequences are listed in Extended Experimental Procedures.

SUPPLEMENTAL INFORMATION

Supplemental Information includes Extended Experimental Procedures, six figures, and one table and can be found with this article online at http://dx.doi.org/10.1016/j.cell.2012.05.032.

ACKNOWLEDGMENTS

We thank S. Nagata, M. Kopf, and R. Adams for generously providing $Mfge8^{-/-}$, $Cd21/35^{-/-}$ and Pdgfrb-Cre mice. S. Luther, H. Zeilhofer, S. Uhlig, T. Suter for materials and reagents. D. Junghans, I. Fischer, M. Nuvolone, T. Chtanova, H. Takizawa, T. Phan, and R. Salomon for discussions. R. Moos, M. Delic, A. Wethmar, N. Wey, S. Behnke, A. Fitsche, S. Walters, K. Webster,

N. Zammit and J.M. Mateos (Center for Microscopy and Image Analysis, University of Zürich) for technical assistance, and R. Kräutler for editing. A. Aguzzi is supported by grants of the European Union (PRIORITY and LUPAS), the Swiss National Foundation (SNF) (one individual award and one Sinergia award with T. Buch and P. Pelczar), the Stammbach Foundation, and the Novartis Research Foundation. A. Aguzzi also holds an Advanced Investigator Grant of the European Research Council. N. Krautler and A. Armulik are supported by the SNF.

Received: November 11, 2011
Revised: March 16, 2012
Accepted: May 11, 2012
Published: July 5, 2012

REFERENCES

Adams, R.H., and Alitalo, K. (2007). Molecular regulation of angiogenesis and lymphangiogenesis. Nat. Rev. Mol. Cell Biol. *8*, 464–478.

Alimzhanov, M.B., Kuprash, D.V., Kosco-Vilbois, M.H., Luz, A., Turetskaya, R.L., Tarakhovsky, A., Rajewsky, K., Nedospasov, S.A., and Pfeffer, K. (1997). Abnormal development of secondary lymphoid tissues in lymphotoxin beta-deficient mice. Proc. Natl. Acad. Sci. USA *94*, 9302–9307.

Aloisi, F., and Pujol-Borrell, R. (2006). Lymphoid neogenesis in chronic inflammatory diseases. Nat. Rev. Immunol. *6*, 205–217.

Armulik, A., Genové, G., and Betsholtz, C. (2011). Pericytes: developmental, physiological, and pathological perspectives, problems, and promises. Dev. Cell *21*, 193–215.

Balogh, P., Aydar, Y., Tew, J.G., and Szakal, A.K. (2001). Ontogeny of the follicular dendritic cell phenotype and function in the postnatal murine spleen. Cell. Immunol. *214*, 45–53.

Blättler, T., Brandner, S., Raeber, A.J., Klein, M.A., Voigtländer, T., Weissmann, C., and Aguzzi, A. (1997). PrP-expressing tissue required for transfer of scrapie infectivity from spleen to brain. Nature *389*, 69–73.

Bofill, M., Akbar, A.N., and Amlot, P.L. (2000). Follicular dendritic cells share a membrane-bound protein with fibroblasts. J. Pathol. *191*, 217–226.

Buch, T., Heppner, F.L., Tertilt, C., Heinen, T.J., Kremer, M., Wunderlich, F.T., Jung, S., and Waisman, A. (2005). A Cre-inducible diphtheria toxin receptor mediates cell lineage ablation after toxin administration. Nat. Methods *2*, 419–426.

Büeler, H.R., Fischer, M., Lang, Y., Bluethmann, H., Lipp, H.P., DeArmond, S.J., Prusiner, S.B., Aguet, M., and Weissmann, C. (1992). Normal development and behaviour of mice lacking the neuronal cell-surface PrP protein. Nature *356*, 577–582.

Cupedo, T., Lund, F.E., Ngo, V.N., Randall, T.D., Jansen, W., Greuter, M.J., de Waal-Malefyt, R., Kraal, G., Cyster, J.G., and Mebius, R.E. (2004). Initiation of cellular organization in lymph nodes is regulated by non-B cell-derived signals and is not dependent on CXC chemokine ligand 13. J. Immunol. *173*, 4889–4896.

Cyster, J.G., Ansel, K.M., Reif, K., Ekland, E.H., Hyman, P.L., Tang, H.L., Luther, S.A., and Ngo, V.N. (2000). Follicular stromal cells and lymphocyte homing to follicles. Immunol. Rev. *176*, 181–193.

De Togni, P., Goellner, J., Ruddle, N.H., Streeter, P.R., Fick, A., Mariathasan, S., Smith, S.C., Carlson, R., Shornick, L.P., Strauss-Schoenberger, J., et al. (1994). Abnormal development of peripheral lymphoid organs in mice deficient in lymphotoxin. Science *264*, 703–707.

Drayton, D.L., Liao, S., Mounzer, R.H., and Ruddle, N.H. (2006). Lymphoid organ development: from ontogeny to neogenesis. Nat. Immunol. *7*, 344–353.

Eberl, G., Marmon, S., Sunshine, M.J., Rennert, P.D., Choi, Y., and Littman, D.R. (2004). An essential function for the nuclear receptor RORgamma(t) in the generation of fetal lymphoid tissue inducer cells. Nat. Immunol. *5*, 64–73.

Finke, D., Acha-Orbea, H., Mattis, A., Lipp, M., and Kraehenbuhl, J. (2002). CD4+CD3- cells induce Peyer's patch development: role of alpha4beta1 integrin activation by CXCR5. Immunity *17*, 363–373.

Foo, S.S., Turner, C.J., Adams, S., Compagni, A., Aubyn, D., Kogata, N., Lindblom, P., Shani, M., Zicha, D., and Adams, R.H. (2006). Ephrin-B2 controls cell motility and adhesion during blood-vessel-wall assembly. Cell *124*, 161–173.

Force, W.R., Walter, B.N., Hession, C., Tizard, R., Kozak, C.A., Browning, J.L., and Ware, C.F. (1995). Mouse lymphotoxin-beta receptor. Molecular genetics, ligand binding, and expression. J. Immunol. *155*, 5280–5288.

Fu, Y.-X., Huang, G., Wang, Y., and Chaplin, D.D. (1998). B lymphocytes induce the formation of follicular dendritic cell clusters in a lymphotoxin alpha-dependent fashion. J. Exp. Med. *187*, 1009–1018.

Fütterer, A., Mink, K., Luz, A., Kosco-Vilbois, M.H., and Pfeffer, K. (1998). The lymphotoxin beta receptor controls organogenesis and affinity maturation in peripheral lymphoid tissues. Immunity *9*, 59–70.

Gaengel, K., Genové, G., Armulik, A., and Betsholtz, C. (2009). Endothelial-mural cell signaling in vascular development and angiogenesis. Arterioscler. Thromb. Vasc. Biol. *29*, 630–638.

Goldman, J.P., Blundell, M.P., Lopes, L., Kinnon, C., Di Santo, J.P., and Thrasher, A.J. (1998). Enhanced human cell engraftment in mice deficient in RAG2 and the common cytokine receptor gamma chain. Br. J. Haematol. *103*, 335–342.

Gretz, J.E., Anderson, A.O., and Shaw, S. (1997). Cords, channels, corridors and conduits: critical architectural elements facilitating cell interactions in the lymph node cortex. Immunol. Rev. *156*, 11–24.

Hanayama, R., Tanaka, M., Miwa, K., Shinohara, A., Iwamatsu, A., and Nagata, S. (2002). Identification of a factor that links apoptotic cells to phagocytes. Nature *417*, 182–187.

Hanayama, R., Tanaka, M., Miyasaka, K., Aozasa, K., Koike, M., Uchiyama, Y., and Nagata, S. (2004). Autoimmune disease and impaired uptake of apoptotic cells in MFG-E8-deficient mice. Science *304*, 1147–1150.

Huber, C., Thielen, C., Seeger, H., Schwarz, P., Montrasio, F., Wilson, M.R., Heinen, E., Fu, Y.X., Miele, G., and Aguzzi, A. (2005). Lymphotoxin-beta receptor-dependent genes in lymph node and follicular dendritic cell transcriptomes. J. Immunol. *174*, 5526–5536.

Humphrey, J.H., Grennan, D., and Sundaram, V. (1984). The origin of follicular dendritic cells in the mouse and the mechanism of trapping of immune complexes on them. Eur. J. Immunol. *14*, 859–864.

Imazeki, N., Senoo, A., and Fuse, Y. (1992). Is the follicular dendritic cell a primarily stationary cell? Immunology *76*, 508–510.

Kamperdijk, E.W., Raaymakers, E.M., de Leeuw, J.H., and Hoefsmit, E.C. (1978). Lymph node macrophages and reticulum cells in the immune response. I. The primary response to paratyphoid vaccine. Cell Tissue Res. *192*, 1–23.

Kapasi, Z.F., Burton, G.F., Shultz, L.D., Tew, J.G., and Szakal, A.K. (1993). Cellular requirements for functional reconstitution of follicular dendritic cells in SCID mice. Adv. Exp. Med. Biol. *329*, 383–386.

Kapasi, Z.F., Qin, D., Kerr, W.G., Kosco-Vilbois, M.H., Shultz, L.D., Tew, J.G., and Szakal, A.K. (1998). Follicular dendritic cell (FDC) precursors in primary lymphoid tissues. J. Immunol. *160*, 1078–1084.

Katakai, T., Suto, H., Sugai, M., Gonda, H., Togawa, A., Suematsu, S., Ebisuno, Y., Katagiri, K., Kinashi, T., and Shimizu, A. (2008). Organizer-like reticular stromal cell layer common to adult secondary lymphoid organs. J. Immunol. *181*, 6189–6200.

Kim, M.Y., Toellner, K.M., White, A., McConnell, F.M., Gaspal, F.M., Parnell, S.M., Jenkinson, E., Anderson, G., and Lane, P.J. (2006). Neonatal and adult CD4+ CD3- cells share similar gene expression profile, and neonatal cells up-regulate OX40 ligand in response to TL1A (TNFSF15). J. Immunol. *177*, 3074–3081.

Kim, M.Y., Rossi, S., Withers, D., McConnell, F., Toellner, K.M., Gaspal, F., Jenkinson, E., Anderson, G., and Lane, P.J. (2008). Heterogeneity of lymphoid tissue inducer cell populations present in embryonic and adult mouse lymphoid tissues. Immunology *124*, 166–174.

Kitamura, D., Roes, J., Kühn, R., and Rajewsky, K. (1991). A B cell-deficient mouse by targeted disruption of the membrane exon of the immunoglobulin mu chain gene. Nature *350*, 423–426.

Klaus, G.G., Humphrey, J.H., Kunkl, A., and Dongworth, D.W. (1980). The follicular dendritic cell: its role in antigen presentation in the generation of immunological memory. Immunol. Rev. *53*, 3–28.

Kranich, J., Krautler, N.J., Heinen, E., Polymenidou, M., Bridel, C., Schildknecht, A., Huber, C., Kosco-Vilbois, M.H., Zinkernagel, R., Miele, G., and Aguzzi, A. (2008). Follicular dendritic cells control engulfment of apoptotic bodies by secreting Mfge8. J. Exp. Med. *205*, 1293–1302.

Le Hir, M., Bluethmann, H., Kosco-Vilbois, M.H., Müller, M., di Padova, F., Moore, M., Ryffel, B., and Eugster, H.P. (1995–1996). Tumor necrosis factor receptor-1 signaling is required for differentiation of follicular dendritic cells, germinal center formation, and full antibody responses. J. Inflamm. *47*, 76–80.

Le Hir, M., Bluethmann, H., Kosco-Vilbois, M.H., Müller, M., di Padova, F., Moore, M., Ryffel, B., and Eugster, H.P. (1996). Differentiation of follicular dendritic cells and full antibody responses require tumor necrosis factor receptor-1 signaling. J. Exp. Med. *183*, 2367–2372.

Lee, I.Y., and Choe, J. (2003). Human follicular dendritic cells and fibroblasts share the 3C8 antigen. Biochem. Biophys. Res. Commun. *304*, 701–707.

Link, A., Vogt, T.K., Favre, S., Britschgi, M.R., Acha-Orbea, H., Hinz, B., Cyster, J.G., and Luther, S.A. (2007). Fibroblastic reticular cells in lymph nodes regulate the homeostasis of naive T cells. Nat. Immunol. *8*, 1255–1265.

Loder, F., Mutschler, B., Ray, R.J., Paige, C.J., Sideras, P., Torres, R., Lamers, M.C., and Carsetti, R. (1999). B cell development in the spleen takes place in discrete steps and is determined by the quality of B cell receptor-derived signals. J. Exp. Med. *190*, 75–89.

Ludewig, B., Odermatt, B., Landmann, S., Hengartner, H., and Zinkernagel, R.M. (1998). Dendritic cells induce autoimmune diabetes and maintain disease via de novo formation of local lymphoid tissue. J. Exp. Med. *188*, 1493–1501.

Mackay, F., and Browning, J.L. (1998). Turning off follicular dendritic cells. Nature *395*, 26–27.

Madisen, L., Zwingman, T.A., Sunkin, S.M., Oh, S.W., Zariwala, H.A., Gu, H., Ng, L.L., Palmiter, R.D., Hawrylycz, M.J., Jones, A.R., et al. (2010). A robust and high-throughput Cre reporting and characterization system for the whole mouse brain. Nat. Neurosci. *13*, 133–140.

Mandel, T.E., Phipps, R.P., Abbot, A., and Tew, J.G. (1980). The follicular dendritic cell: long term antigen retention during immunity. Immunol. Rev. *53*, 29–59.

Mebius, R.E. (2003). Organogenesis of lymphoid tissues. Nat. Rev. Immunol. *3*, 292–303.

Mebius, R.E., Rennert, P., and Weissman, I.L. (1997). Developing lymph nodes collect CD4+CD3- LTbeta+ cells that can differentiate to APC, NK cells, and follicular cells but not T or B cells. Immunity *7*, 493–504.

Mombaerts, P., Iacomini, J., Johnson, R.S., Herrup, K., Tonegawa, S., and Papaioannou, V.E. (1992). RAG-1-deficient mice have no mature B and T lymphocytes. Cell *68*, 869–877.

Moro, K., Yamada, T., Tanabe, M., Takeuchi, T., Ikawa, T., Kawamoto, H., Furusawa, J., Ohtani, M., Fujii, H., and Koyasu, S. (2010). Innate production of T(H)2 cytokines by adipose tissue-associated c-Kit(+)Sca-1(+) lymphoid cells. Nature *463*, 540–544.

Motegi, S., Garfield, S., Feng, X., Sárdy, M., and Udey, M.C. (2011a). Potentiation of platelet-derived growth factor receptor-β signaling mediated by integrin-associated MFG-E8. Arterioscler. Thromb. Vasc. Biol. *31*, 2653–2664.

Motegi, S., Leitner, W.W., Lu, M., Tada, Y., Sárdy, M., Wu, C., Chavakis, T., and Udey, M.C. (2011b). Pericyte-derived MFG-E8 regulates pathologic angiogenesis. Arterioscler. Thromb. Vasc. Biol. *31*, 2024–2034.

Ngo, V.N., Cornall, R.J., and Cyster, J.G. (2001). Splenic T zone development is B cell dependent. J. Exp. Med. *194*, 1649–1660.

Ngo, V.N., Korner, H., Gunn, M.D., Schmidt, K.N., Riminton, D.S., Cooper, M.D., Browning, J.L., Sedgwick, J.D., and Cyster, J.G. (1999). Lymphotoxin alpha/beta and tumor necrosis factor are required for stromal cell expression of homing chemokines in B and T cell areas of the spleen. J. Exp. Med. *189*, 403–412.

Pasparakis, M., Alexopoulou, L., Episkopou, V., and Kollias, G. (1996). Immune and inflammatory responses in TNF alpha-deficient mice: a critical requirement for TNF alpha in the formation of primary B cell follicles, follicular dendritic cell networks and germinal centers, and in the maturation of the humoral immune response. J. Exp. Med. *184*, 1397–1411.

Pasparakis, M., Kousteni, S., Peschon, J., and Kollias, G. (2000). Tumor necrosis factor and the p55TNF receptor are required for optimal development of the marginal sinus and for migration of follicular dendritic cell precursors into splenic follicles. Cell. Immunol. *201*, 33–41.

Phan, T.G., Grigorova, I., Okada, T., and Cyster, J.G. (2007). Subcapsular encounter and complement-dependent transport of immune complexes by lymph node B cells. Nat. Immunol. *8*, 992–1000.

Picarella, D.E., Kratz, A., Li, C.B., Ruddle, N.H., and Flavell, R.A. (1992). Insulitis in transgenic mice expressing tumor necrosis factor beta (lymphotoxin) in the pancreas. Proc. Natl. Acad. Sci. USA *89*, 10036–10040.

Rennert, P.D., James, D., Mackay, F., Browning, J.L., and Hochman, P.S. (1998). Lymph node genesis is induced by signaling through the lymphotoxin beta receptor. Immunity *9*, 71–79.

Strick-Marchand, H., Masse, G.X., Weiss, M.C., and Di Santo, J.P. (2008). Lymphocytes support oval cell-dependent liver regeneration. J. Immunol. *181*, 2764–2771.

Suematsu, S., and Watanabe, T. (2004). Generation of a synthetic lymphoid tissue-like organoid in mice. Nat. Biotechnol. *22*, 1539–1545.

Takatori, H., Kanno, Y., Watford, W.T., Tato, C.M., Weiss, G., Ivanov, I.I., Littman, D.R., and O'Shea, J.J. (2009). Lymphoid tissue inducer-like cells are an innate source of IL-17 and IL-22. J. Exp. Med. *206*, 35–41.

Tang, W., Zeve, D., Suh, J.M., Bosnakovski, D., Kyba, M., Hammer, R.E., Tallquist, M.D., and Graff, J.M. (2008). White fat progenitor cells reside in the adipose vasculature. Science *322*, 583–586.

Tew, J.G., Thorbecke, G.J., and Steinman, R.M. (1982). Dendritic cells in the immune response: characteristics and recommended nomenclature (A report from the Reticuloendothelial Society Committee on Nomenclature). J. Reticuloendothel. Soc. *31*, 371–380.

Tian, Y., Chen, J., Gaspert, A., Segerer, S., Clavien, P.A., Wüthrich, R.P., and Fehr, T. (2010). Kidney transplantation in mice using left and right kidney grafts. J. Surg. Res. *163*, e91–e97.

Tumanov, A.V., Kuprash, D.V., Mach, J.A., Nedospasov, S.A., and Chervonsky, A.V. (2004). Lymphotoxin and TNF produced by B cells are dispensable for maintenance of the follicle-associated epithelium but are required for development of lymphoid follicles in the Peyer's patches. J. Immunol. *173*, 86–91.

Ware, C.F., Crowe, P.D., Grayson, M.H., Androlewicz, M.J., and Browning, J.L. (1992). Expression of surface lymphotoxin and tumor necrosis factor on activated T, B, and natural killer cells. J. Immunol. *149*, 3881–3888.

Wilke, G., Steinhauser, G., Grün, J., and Berek, C. (2010). In silico subtraction approach reveals a close lineage relationship between follicular dendritic cells and BP3(hi) stromal cells isolated from SCID mice. Eur. J. Immunol. *40*, 2165–2173.

Yoshida, T., and Takaya, K. (1989). Follicular dendritic reticular cells in the germinal center of the rat lymph node as studied by immuno-electron microscopy. Arch. Histol. Cytol. *52*, 327–335.

Zhang, N., Guo, J., and He, Y.W. (2003). Lymphocyte accumulation in the spleen of retinoic acid receptor-related orphan receptor gamma-deficient mice. J. Immunol. *171*, 1667–1675.